Molecular Cell, Volume *67*

Supplemental Information

PP2A Controls Genome Integrity by Integrating Nutrient-Sensing and Metabolic Pathways with the DNA Damage Response

Elisa Ferrari, Christopher Bruhn, Marta Peretti, Corinne Cassani, Walter Vincenzo Carotenuto, Mohamed Elgendy, Ghadeer Shubassi, Chiara Lucca, Rodrigo Bermejo, Mario Varasi, Saverio Minucci, Maria Pia Longhese, and Marco Foiani

INVENTORY OF SUPPLEMENTARY INFORMATION

Supplemental Figures

Figure S1, Related to Figure 1. *IRC21* deletion rescues checkpoint mutants.
Figure S2, Related to Figure 3. Irc21 interacts with PP2A and PP2A-like phosphatases.
Figure S3, Related to Figure 3. Irc21 interacts with PP2A and PP2A-like phosphatases.
Figure S4, Related to Figure 4. PP2A mutants rescue checkpoint defects.
Figure S5, Related to Figure 5. Irc21 exerts PP2A-dependent and PP2A-activating metabolic regulations.
Figure S6, Related to Figure 6. Ceramides, TORC1 and Ppm1 impact on the HU-induced DDR by modulating PP2A activity.

Supplemental Tables

Table S1, Yeast strains used in this study, related to STAR Methods.
See excel File Table S1.
Table S2, Primer sequences used in this study, related to STAR Methods.
See excel File Table S2.

Figure S1, Related to Figure 1. *IRC21* deletion rescue checkpoint mutants.

(A,B,D) Cells were grown on YPD plates +/- HU (Figure S1D: a superfluous part of the plates was digitally eliminated).

(C) Cells were arrested in G_1 with α-factor (αF) and released into YPD containing 0.2 M HU. After 3 hours, cells were released into YPD. Samples were collected at

the indicated times to determine DNA content by fluorescence-activated cell sorting (FACS) analysis (Related to Figure 1D).

(E) Cells were arrested with α-factor and released in YPD or YPD containing 0.2 M HU. Cells were treated for 3 hours and harvested to detect Dun1 and Rad53.

(F) Cells were arrested in G_1 with α-factor and released into YPD containing 0.2 M HU. After 3 hours, cells were released into YPD. Samples were collected at the indicated times to determine DNA content by fluorescence-activated cell sorting (FACS) analysis (left panel) and to detect Rad53, Dun1, P-H2A and H2A by Western blot analysis (right panel).

Figure S2, Related to Figure 3. Irc21 interacts with PP2A and PP2A-like phosphatases.

(A) Top 10 array mutants with highest interactome similarity to *irc21*Δ. The Pearson correlation (R) value was obtained by comparing the interactome of the *irc21*Δ array strain with the interactomes of 3884 mutant array strains with the 1712 query mutants (datasets from (Costanzo et al., 2010)). (Related to Figure 3A).

(B) Negative and rescuing genetic interactions of *IRC21* assessed by SGA screening. Left panel: Quantitative effect of array gene deletions (rows) on the growth of *irc21*Δ mutants vs. wt. Middle panel: Manual functional classification of *IRC21* interactors. Right panel: Comparison with published SGA scores (Costanzo et al., 2010).

Figure S3, Related to Figure 3. Irc21 interacts with PP2A and PP2A-like phosphatases.

(A) Epistatic genetic interactions of *IRC21* assessed by SGA screening. Left panel: Quantitative effect of array gene deletions (rows) on the growth of *irc21Δ* mutants vs. wt. Middle panel: Manual functional classification of *IRC21* interactors. Right panel: Comparison with published SGA scores (Costanzo et al., 2010).

(B) Tetrad analysis of *irc21Δ rrd1Δ*, *irc21Δ ptc1Δ*, *irc21Δ rts1Δ*, *irc21Δ tip41Δ*, *irc21Δ sap190Δ* strains (Related to Figure 3D).

(C) Confirmation of the genetic interactions between Irc21 and Rrd1, Ptc1 and Rts1 by random spore analysis (spore derived from the SGA screening, performed in S228C genetic background) (Related to Figure 3D).

Figure S4, Related to Figure 4. PP2A mutants rescue checkpoint defects.

(A) Cells were grown on SD/-Ura containing glucose 2% or galactose 2% +/- HU.

(B) Cells were grown on YPD plates +/- HU.

(C) Cells were grown on YPD plates +/- rapamycin or metformin.

(D) Cells were treated for 30' with 200ng/ml rapamycin. Bandshift assays following the phosphorylation of PP2A branch proteins Gln3, Nnk1, and Npr1.

Figure S5, Related to Figure 5. Irc21 exerts PP2A-dependent and PP2A-activating metabolic regulations.

(A) Quantification (pmol/mg) of the listed metabolites in wt and *irc21Δ* cells by TrueMass Ceramide analysis. Average values (AVG), standard deviation (SD) and standard error of the mean (SEM) are shown (Related to Figures 5D and E).

(B) TrueMass Ceramide panel quantification of the listed metabolites in *irc21*Δ cells. *p*-value and statistical significance are shown (Related to Figures 5D and E).

(C) Illustration of sphingolipid biosynthesis in *S. cerevisiae*. Colored metabolites indicate an increase (red) or a decrease (green) of their amount in *irc21Δ* cells (refer to Figure S5B). Myriocin inhibits serine palmitoyl-CoA transferase. Fumonisin B1 inhibits ceramide synthase.

(D) Cell sensitivity to syringomycin in presence or absence of dihydroceramide. Cells were grown in SD medium. Average values are shown and error bars represent the standard deviation.

(E) *mec1Δ sml1Δ irc21Δ* cells were arrested in G_1 with α-factor and released into YPD containing 0.1 M HU. After 3 hours, cells were released into YPD or YPD with ceramide 15μM. Samples were collected at the indicated times to detect Rad53, by Western blot analysis.

Figure S6, Related to Figure 6. Ceramides, TORC1 and Ppm1 impact on the HU-induced DDR by modulating PP2A activity.

(A) Cells were treated with 200ng/ml rapamycin. Bandshift assays following the phosphorylation of PP2A branch proteins Gln3, Nnk1, Npr1 and Rtg3, after 30' of rapamycin treatment.

(B) Cells were treated with 0.2M HU alone or in combination with rapamycin 200ng/ml, ceramide 15μM, rapamycin 200ng/ml + ceramide 15μM. Samples were collected at the indicated times to determine DNA content by FACS analysis, to detect Rad53 and Nnk1 by Western blot analysis, to evaluate the budding index.

Figure S1, related to Figure1

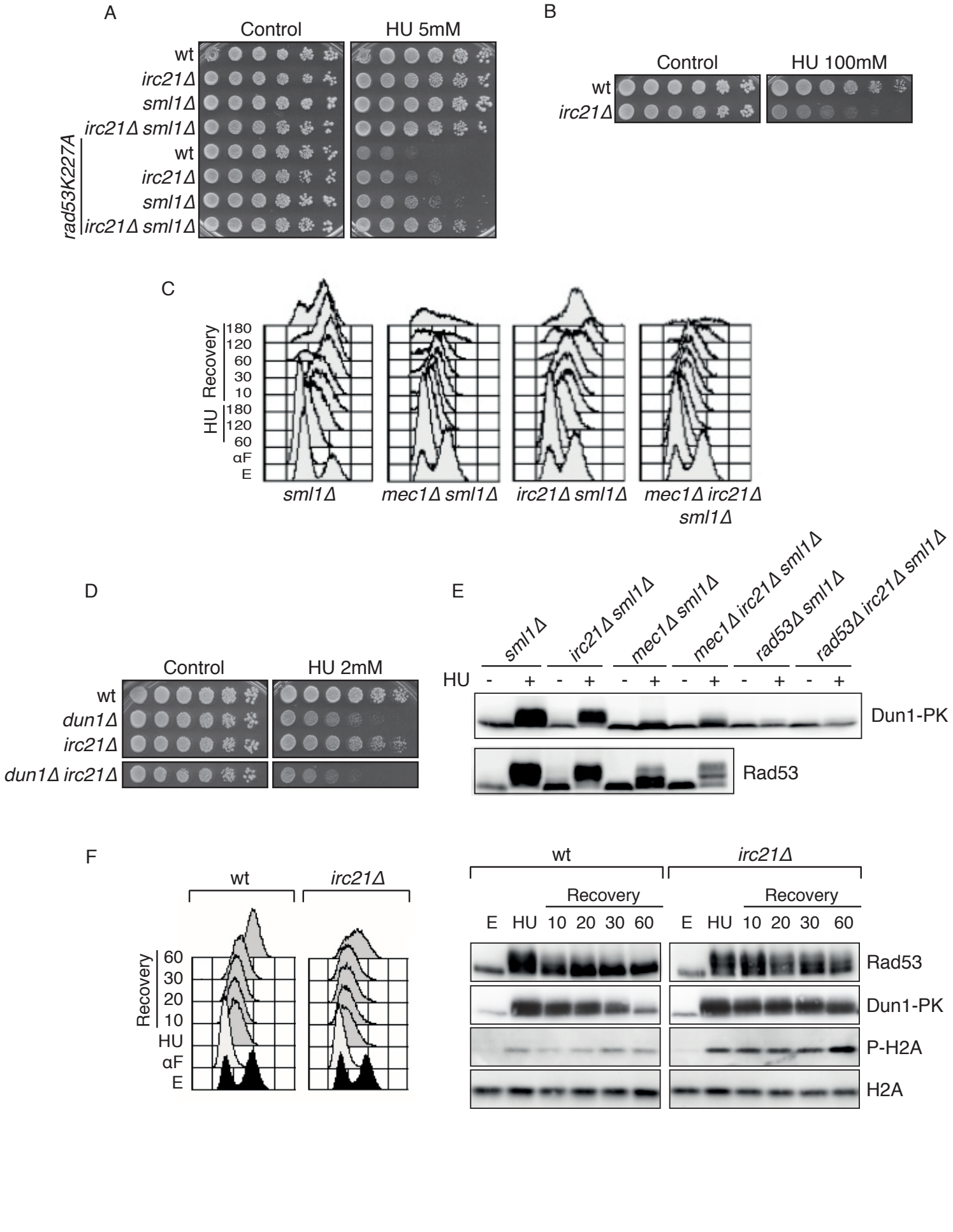

Figure S2, related to Figure 3

A

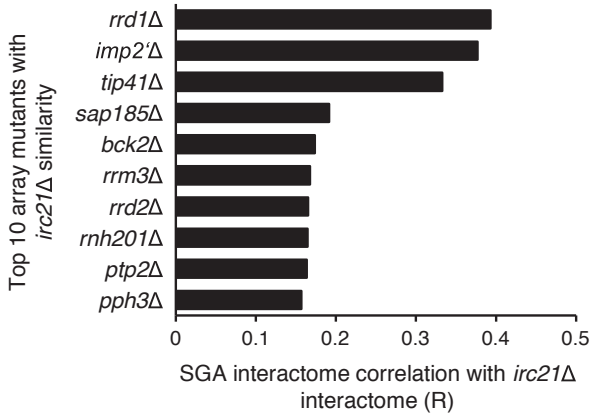

B

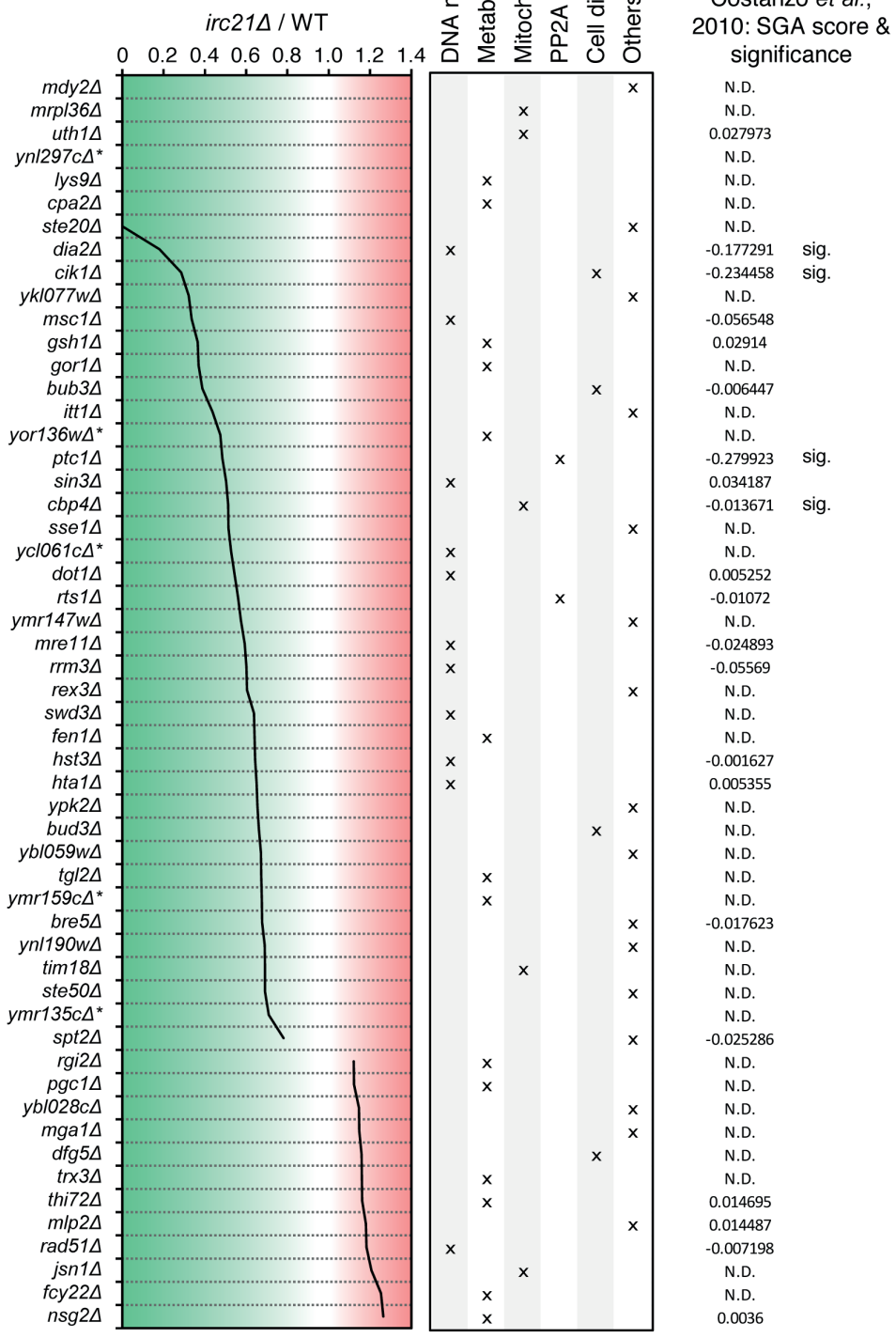

Figure S3, related to Figure 3

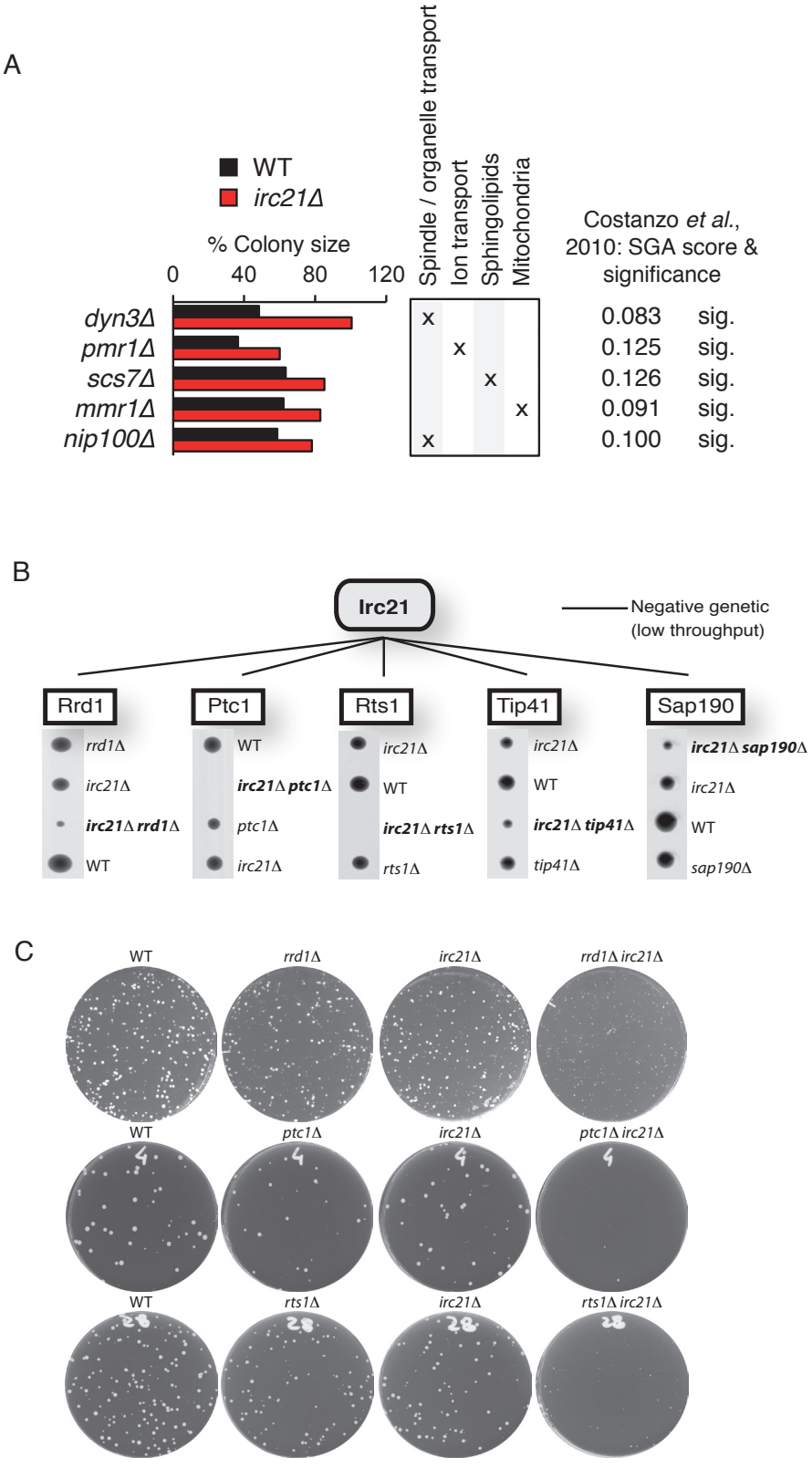

Figure S4, related to Figure 4

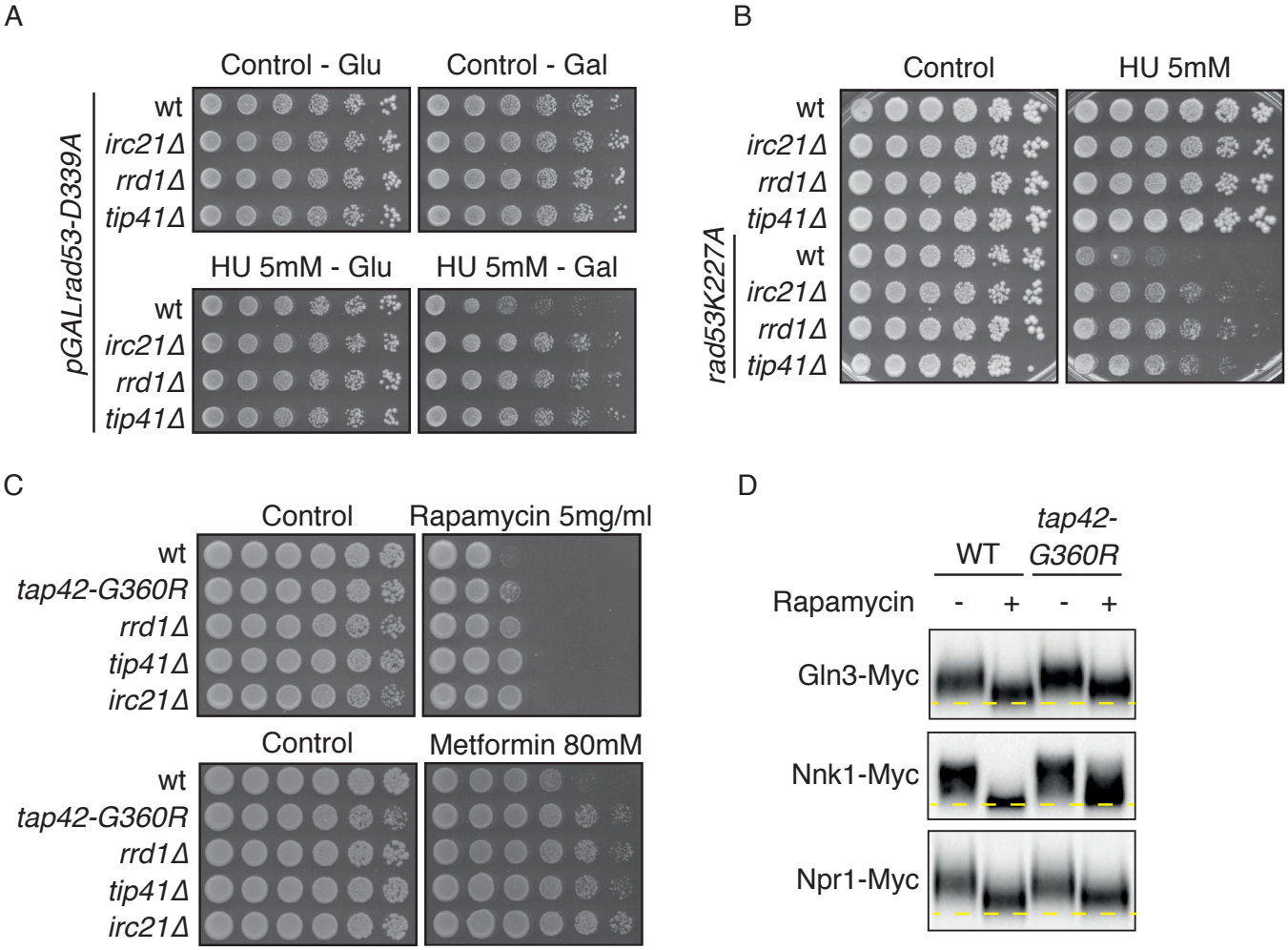

Figure S5, related to Figure 5

A

	AVG		SD		SEM	
	wt	*irc21Δ*	wt	*irc21Δ*	wt	*irc21Δ*
3-ketodihydrosphingosine	0.39608	1.48481	0.08514	0.16890	0.0301	0.0755
ceramide-1-P	0.00057	0.00059	0.00032	0.00021	0.0001	0.0001
phytoceramide	0.01393	0.01695	0.00745	0.00581	0.0026	0.0026
dihydroceramide	0.34901	0.10606	0.27825	0.04989	0.0984	0.0223
sphingosine-1-phosphate	0.00153	0.00264	0.00077	0.00100	0.0003	0.0004
dihydrosphingosine	3.30267	6.05759	0.64619	0.54065	0.2285	0.2418
dihydrosphingosine-1-P	0.13061	0.71767	0.09609	0.20008	0.0340	0.0895
sphingosine	0.15799	0.20003	0.04349	0.08096	0.0154	0.0362

B

Metabolite	p-value	significance
3-ketodihydrosphingosine	0.0034	**
ceramide-1-P	0.08836	
phytoceramide	0.2128	
dihydroceramide	0.0187	*
sphingosine-1-phosphate	0.0773	
dihydrosphingosine	0.0033	**
dihydrosphingosine-1-P	0.0034	**
sphingosine	0.2716	

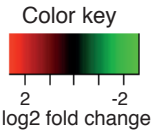

C

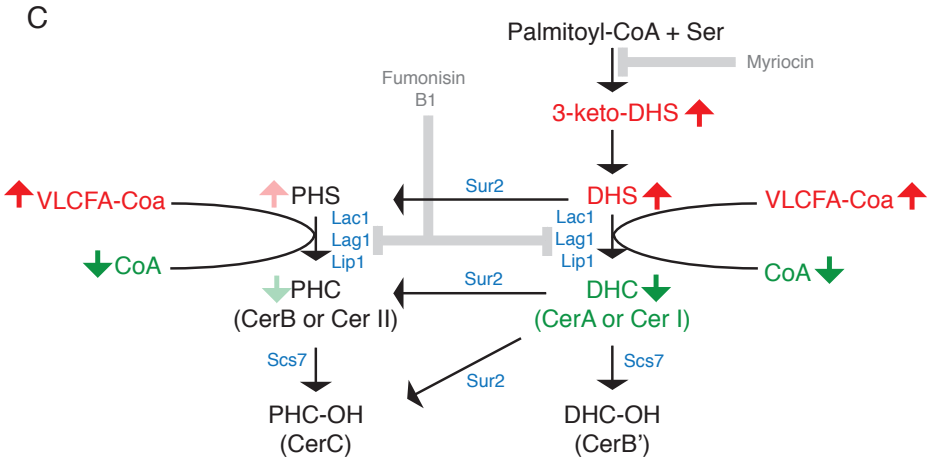

D

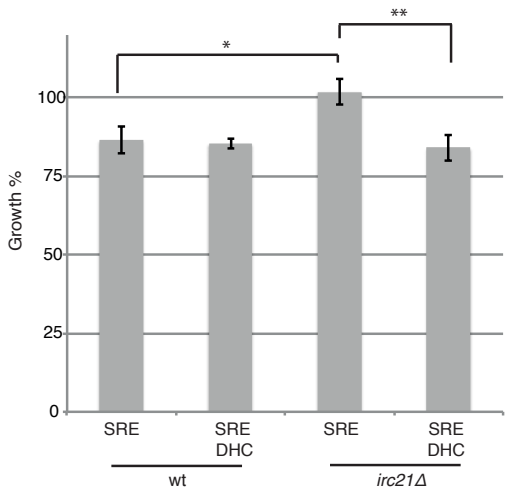

E

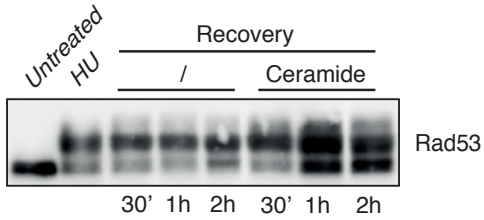
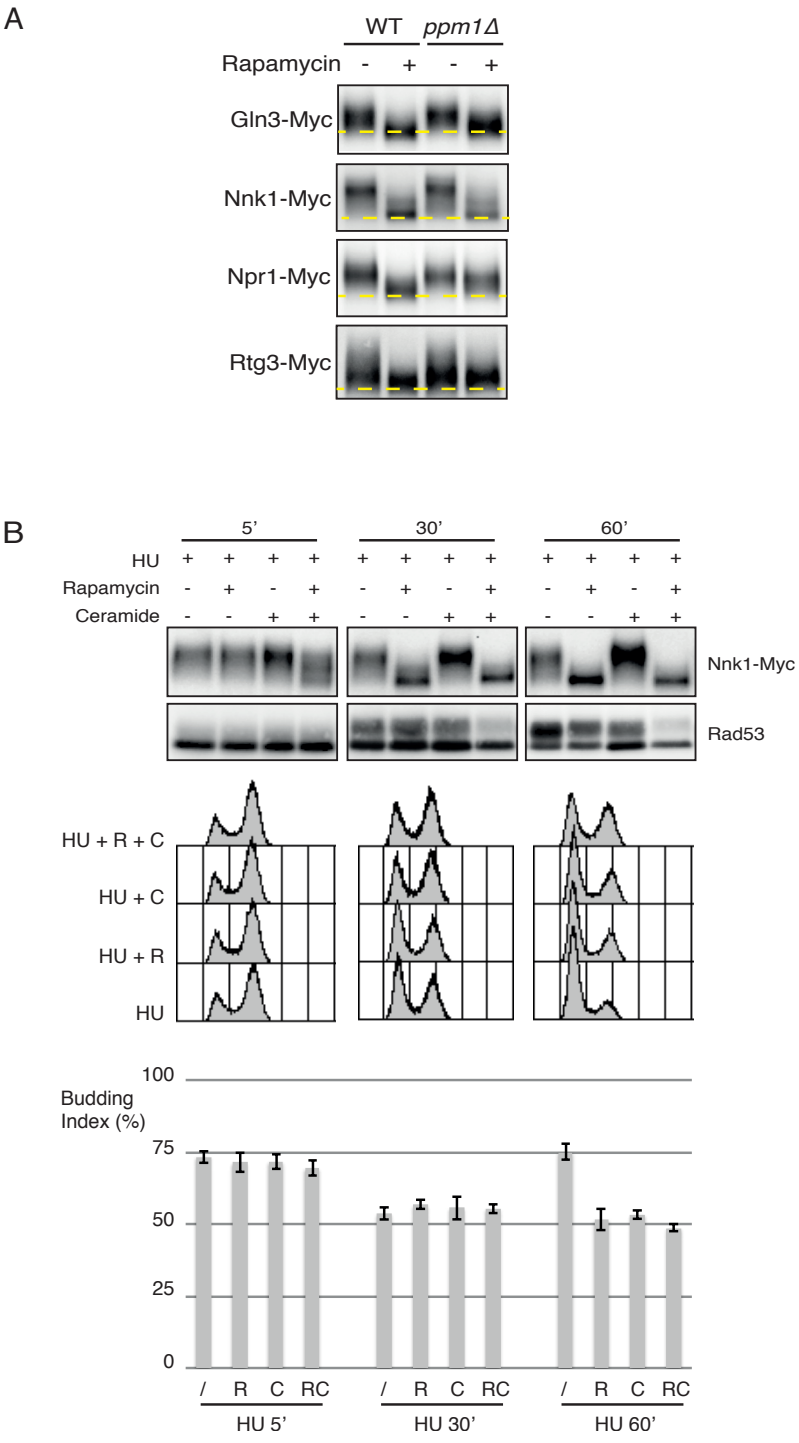
Figure S6, related to Figure 6